# Quantized Radio Map Estimation Using Tensor and Deep Generative Models

Subash Timilsina

PhD Qualification Exam
Oregon State University

**Advisor:** Xiao Fu

November 7, 2023

# Motivation

src: https://en.wikipedia.org/wiki/Reser_Stadium

**Spectrum scarcity in crowded places:**

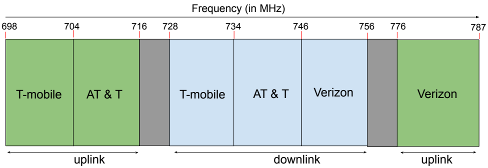


Spectrum bands of few carriers in US.

- Cell phones use distinct frequency channels.
- Slow internet and dropped calls due to high demand.

# Motivation

- Frequency bands $\leftrightarrow$ Highways or lanes.

src:https://www.bbc.com/news/health-38506735.

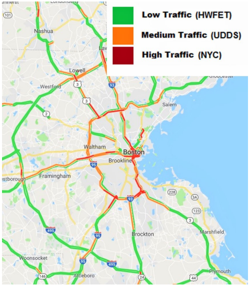


What could help us?

# Motivation

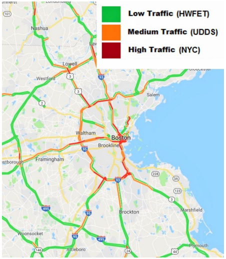


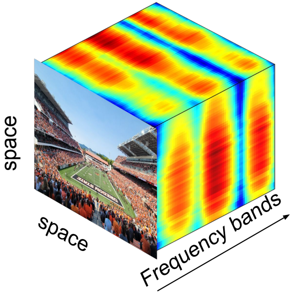


src: image on left [Houshmand et al. 2018]

- Radio map $\leftrightarrow$ Google map.
- Helps to see the busy and free spectrum.

**Spectrum cartography**

- Just as GPS helps navigating maps, spectrum cartography helps us create radio maps.

# Why Spectrum Cartography?

**Why do we want to construct such map?**

- **Applications:** Wireless resources allocation, interference management, spectrum surveillance, and so on [Ball et al. 2005; Bi et al. 2019; Höyhtyä et al. 2012].

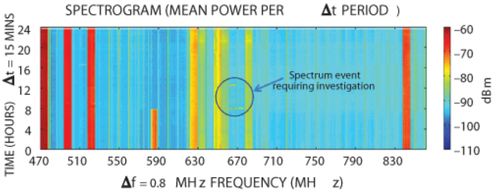


Spectrum surveillance; src: https://www.microwavejournal.com/articles/18089

# Importance of Spectrum Cartography

**Who wants this?**

- Government agencies and labs for regulations.

Federal Communication Commission [Spectrum et al. 2023a]


Institute for Telecommunication [Spectrum et al. 2023b]

**Commercial companies:**

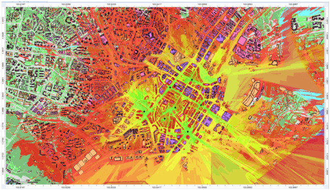

Radio map of city in Singapore. src: LuxCarta [LuxCarta 2023]


RemCom [RemCom 2023]

- Telecommunication companies use SC for generating their coverage map.

It is a widely studied problem in wireless communications [Bazerque et al. 2011; Boccolini et al. 2012; Jayawickrama et al. 2013; Kim et al. 2013; Mateos et al. 2009; Shrestha et al. 2022; Teganya et al. 2020; Zhang et al. 2020].

# Spectrum Cartography/Radio map estimation

Emitters

Sensors

**Emitters:**

- Transmits signals in the range of radio frequency (RF) spectrum.

**Sensors:**

- Can measure and detect RF signals in different frequencies.

**Power spectral density (PSD):**

- Distribution of power in a signal spread out over various frequency components.

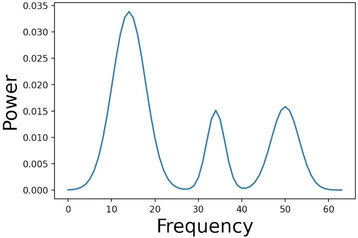

# Spectrum Cartography

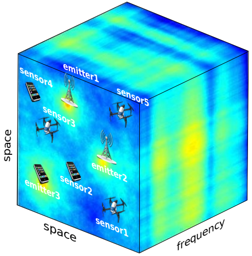


src:[Shrestha et al. 2022]

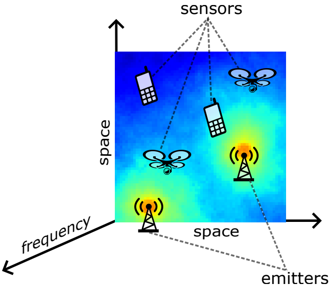


**Radio map/Power propagation map:**

- Power spectral density map that displays power of signal at different locations and frequency.

**Spectrum Cartography (SC):**

- Constructing radio map to understand the allocation and usage of different frequencies in the space.

# Spectrum Cartography Scenario

**Sensing Scenario:**

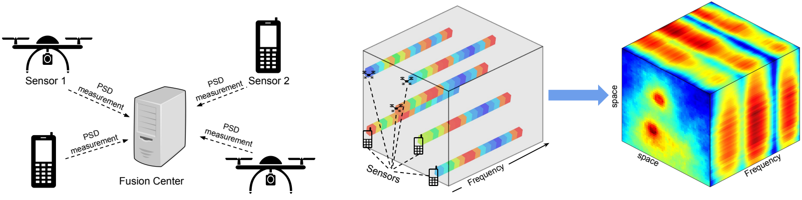


Sparse PSD measurements

Full radio map

- Sensors collect the PSD measurements from different locations.
- Sparse measurements are send to fusion center.

**Goal:**

- Construct radio map across multiple domain using limited number of power spectral density (PSD) measurements from sensors.

# Problem statement: Spectrum Cartography

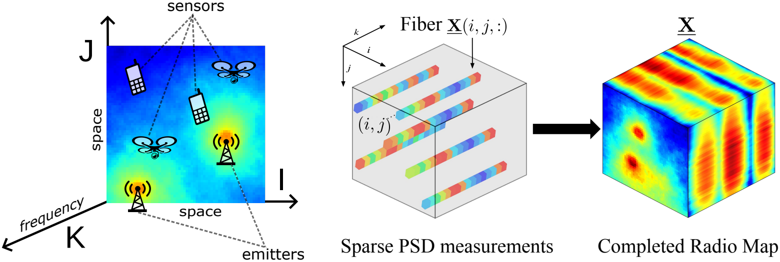


**Setting:**

- $R$ emitters emitting radio signals across $K$ frequency bins, $N$ sensors deployed on $I \times J$ space sending measurement to fusion center.
- Set of sensor locations $\boldsymbol{\Omega} = \{\ (i,j) \mid i \in [I], j \in [J]\ \}$ and $|\boldsymbol{\Omega}| = N \ll IJ$.
- Each sensor at $(i,j)$ collects measurements $\underline{\boldsymbol{X}}(i,j,:)$ which is a tensor fiber.

**Goal:**

- Recover tensor $\underline{\boldsymbol{X}} \in \mathbb{R}^{I\times J\times K}$, full radio map at fusion center from limited sensor measurements $\{\underline{\boldsymbol{X}}(i,j,:)\}_{(i,j)\in\boldsymbol{\Omega}}$.

**Challenges:**

- Estimating a high-dimensional tensor from few observations is an ill-posed problem.

## Early Methods and Challenges

- Treat SC as an image inpainting problem.

- **Kriging Interpolation** [Boccolini et al. 2012]
  - Uses the idea that closer points are more similar than distant ones.
  - Computes weights from sampled measurements to interpolates value at unsampled measurements.
  - Works if have enough number of representative samples.

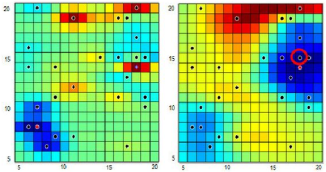


Krigging interpolation; src:[Maurand et al. 2014]

- **Thin Plate Spline** [Bazerque et al. 2011; Hamid et al. 2017]
  - Fits measurements with continuous and smooth curves.
  - Interpolates using the fitted function.
  - Works if the power propagation is smooth.

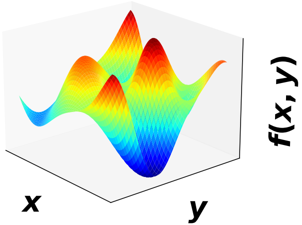


**Challenges:**

- Requires smooth power distribution.
- Doesn't provide any recoverability analysis.
- Limited to 1 frequency band.
  - Work with a single frequency band i.e. 2D maps.
  - Processing 3D maps requires handling each frequency band as a separate 2D map.

# Radio Map Model

- Radio map can be decomposed into the latent factors associated with spatial and spectral information [Bazerque et al. 2011; Romero et al. 2017; Shrestha et al. 2022; Zhang et al. 2020],

$$\underline{\boldsymbol{X}}(i,j,k)=\sum_{r=1}^{R}\boldsymbol{S}_r(i,j)\boldsymbol{c}_r(k)\Longleftrightarrow\underline{\boldsymbol{X}}=\sum_{r=1}^{R}\boldsymbol{S}_r\circ\boldsymbol{c}_r. \qquad (1)$$

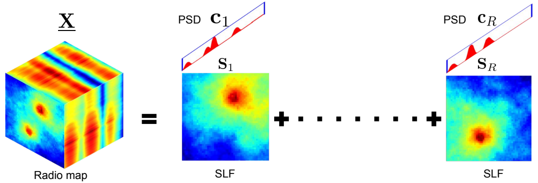


where, $\boldsymbol{S}_r\in\mathbb{R}^{I\times J}$ is the **Spatial loss field (SLF)** of $r$-th emitter:

- captures the power distribution over the space due to an emitter,

and $\boldsymbol{c}_r\in\mathbb{R}^{K}$ is the **Power spectral density (PSD)** of $r$-th emitter:

- reflects the power of the signal over various frequencies transmitted by emitter.

# Low-rank Block-term Tensor Decomposition (BTD) model:

- Recent work in [Zhang et al. 2020] proposed low-rank BTD.
- Model SLF of an $r-$th emitter as low rank matrix $\boldsymbol{S}_r = \boldsymbol{A}_r \boldsymbol{B}_r^\top$ where $\boldsymbol{A}_r \in \mathbb{R}^{I \times L}$, $\boldsymbol{B}_r \in \mathbb{R}^{J \times L}$ with $\operatorname{rank}(\boldsymbol{A}_r) = \operatorname{rank}(\boldsymbol{B}_r) = L \ll \min(I, J)$.

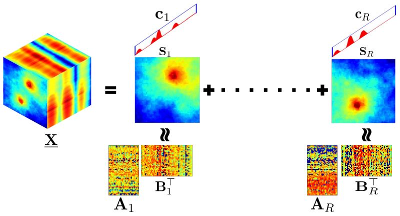


- Obtains full radio map using following criterion [Zhang et al. 2020],

$$\underset{\{\boldsymbol{c}_r, \boldsymbol{A}_r, \boldsymbol{B}_r\}_{r=1}^R}{\text{minimize}} \left\| \underline{\boldsymbol{M}}_{\text{sens}} \circledast \left( \underline{\boldsymbol{X}} - \sum_{r=1}^{R} (\boldsymbol{A}_r \boldsymbol{B}_r^\top) \circ \boldsymbol{c}_r \right) \right\|_{\mathrm{F}}^2, \qquad (2)$$

where $\underline{\boldsymbol{M}}_{\text{sens}}$ is a sensing mask tensor such that $\underline{\boldsymbol{M}}_{\text{sens}}(i,j,:) = \boldsymbol{1}$ if $(i,j) \in \boldsymbol{\Omega}$ and $\underline{\boldsymbol{M}}_{\text{sens}}(i,j,:) = \boldsymbol{0}$ otherwise.

# Challenges of Early Methods

- Using methods such as low rankness [Zhang et al. 2020] fails in presence of heavy shadowing.

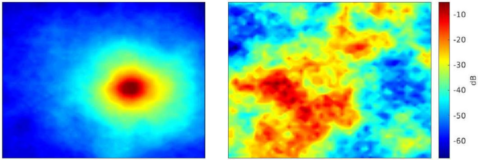


Low shadowing Heavy shadowing

src: [Shrestha et al. 2022]

**Shadowing:**

- **Cause:** when there is interference of radio signals.
- **Low shadowing:** smooth radio map due to absence of obstacles; power distribution is even.
- **Heavy Shadowing:** uneven radio map due to obstacles; common in indoor environments.

# Challenges of Early Methods

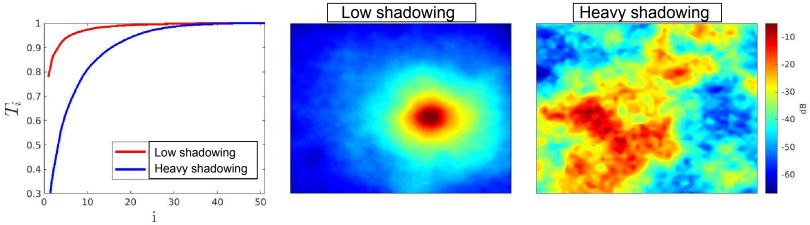


src: [Shrestha et al. 2022]

- $T_i = \frac{\sum_{k=1}^{i} \mu_k}{\sum_{k=1}^{51} \mu_k}$ under different shadowing scenarios where $\mu_k$ is $k$th largest singular value.

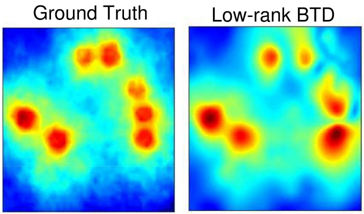


src: [Shrestha et al. 2022]

# Deep Completion Methods

- Train a DNN to predict whole radio map $\underline{\boldsymbol{X}}$ [Han et al. 2020; Teganya et al. 2020].

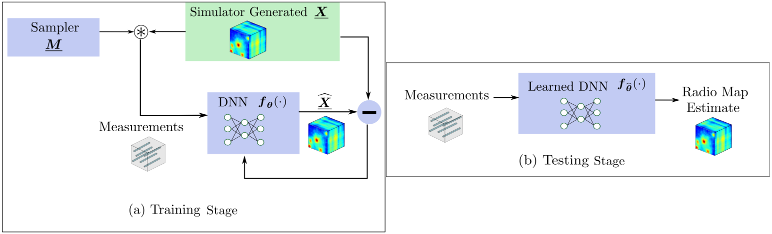


[Teganya et al. 2020]

**Challenges:**

- Costly training stage of these models.
  - If $R \leq 5$ and $I = J = 100$, the number of different emitter locations exceeds $8 \times 10^{17}$ [Shrestha et al. 2022].
- Poses generalization challenges as the training samples might not cover the most representative samples [Shrestha et al. 2022].

# Deep Generative Models (DGM) as Individual SLF:

- Model individual SLF with deep generative model [Shrestha et al. 2022], i.e., $\underline{\boldsymbol{S}_r = \boldsymbol{g}_{\boldsymbol{\theta}}(\boldsymbol{z}_r) \in \mathbb{R}^{I \times J}}$ where,
  - $\boldsymbol{g}_{\boldsymbol{\theta}}(\cdot)$ is the generative model pre-trained on various SLFs,
  - $\boldsymbol{z}_r \in \mathbb{R}^D$ is the latent embedding.
- Can model heavy shadowing scenario.
- Using $I = J = 100$, there are $10^4$ possible emitter location.

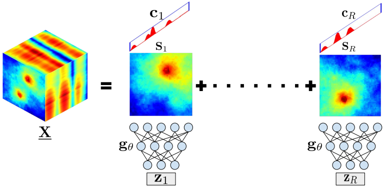


- Optimize following objective,

$$\underset{\{\boldsymbol{c}_r, \boldsymbol{z}_r\}_{r=1}^{R}}{\text{minimize}} \left\| \underline{\boldsymbol{M}}_{\text{sens}} \circledast \left( \underline{\boldsymbol{X}} - \sum_{r=1}^{R} \boldsymbol{g}_{\boldsymbol{\theta}}(\boldsymbol{z}_r) \circ \boldsymbol{c}_r \right) \right\|_{\text{F}}^{2}. \tag{3}$$

# Comparisons and Observations

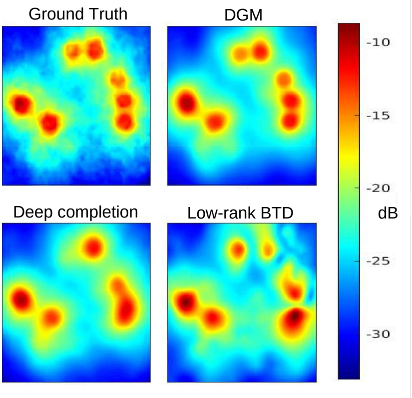


src: [Shrestha et al. 2022]

**Key Observations:**

- Modeling SLF with a deep priors [Shrestha et al. 2022] are effective compared to previous methods and show promising results.
- However all these methods uses real-valued measurements.

# Problem With Using Real-valued Measurements

Using **real-valued measurements** is not feasible in practice [Konar et al. 2014; Mehanna et al. 2013].

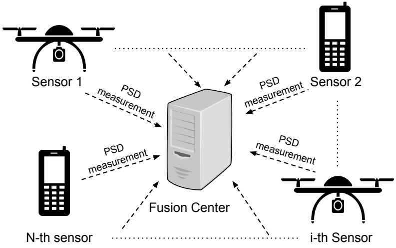


- **Increased data volume:** Communication overhead in large sensor networks.
- **Bandwidth constraints:** Limited bandwidth can lead to network congestion.
- **Energy consumption:** Increases the energy consumption in battery-operated sensors.
- **Latency:** Increases latency, impacting the real-time data collection.

# Existing Solution

- What happens when we treat quantized measurements as real-valued measurements in existing methods?

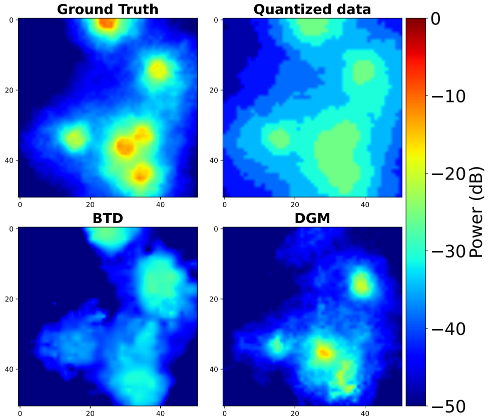

# Existing Framework for Quantized Data:

- [Romero et al. 2017] proposed kernel regression for SC with quantized measurements.
- Optimize following objective,

$$\underset{\{\boldsymbol{b}\in\mathbb{R}^N\}_{r=1}^R}{\text{minimize}} \sum_{(i,j)\in\boldsymbol{\Omega}} \sum_{k=1}^{K} \left( \mathcal{G}(\underline{\boldsymbol{X}}(i,j,k)) - \sum_{r=1}^{R} \boldsymbol{S}_r(i,j,k)\ \boldsymbol{c}_r(k) \right)^2. \qquad (4)$$

where,

$$\boldsymbol{S}_r = \sum_{\ell=1}^{N} \boldsymbol{K}\left(\mathcal{G}(\underline{\boldsymbol{X}}(i,j,k)),\ x_\ell\right) \boldsymbol{b}_\ell, \quad \boldsymbol{K}\left(x_i, x_n\right) = \frac{\|x_i - x_n\|_2^2}{\sigma^2}$$

$x_\ell$ is the $\ell$-th observation,

$\mathcal{G}(\cdot)$ is the quantizer and $\sigma$ is the bandwidth of Gaussian kernel.

- Assumes that the fusion center has knowledge of the PSDs of emitters.
- Unrealistic assumption because estimating PSDs of an emitters is highly nontrivial problem [Fu et al. 2015, 2016].

# Objective

How do we design a method that reconstruct the radio map with **quantized** and **limited measurements** with **heavy shadowing** scenario ?

- Quantized tensor recovery problem.

# Challenges of problem

- Although quantized tensor recovery problem has been studied in literature [Ghadermarzy et al. 2018; Lee et al. 2020; Li et al. 2018].

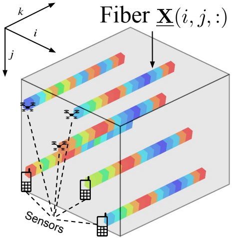


**Additional challenges:**

- Fiber sampling of tensor.
- Tensor modeling with DGM and BTD.

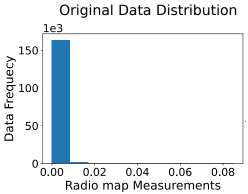


- Small power values and skewed distributions in radio map measurements poses challenges in quantization.

# Quantization Strategy

**Quantization at sensors:**

- Employ $\underline{\text{Gaussian quantization at the sensors}}$ that is widely used [Bhaskar 2016; Cao et al. 2015; Davenport et al. 2014; Ghadermarzy et al. 2018; Lee et al. 2020; Li et al. 2018; McCullagh 1980]:

$$\underline{\boldsymbol{Y}}(i,j,:) = \mathcal{G}(\ h(\underline{\boldsymbol{X}}(i,j,;)) + \underline{\boldsymbol{V}}\ )$$
$$\mathcal{G}(x) = q,\ \text{if } b_{q-1} < x \leq b_q, \quad q \in [Q] = \{1, ..., Q\},$$

**Measurement:**

- $\underline{\boldsymbol{X}}(i,j,;)$ is sensor measurement at location $(i,j) \in \boldsymbol{\Omega}$,

**Transformation:**

- $h(x) = \log(x + a)$ element-wise with $a > 0$.

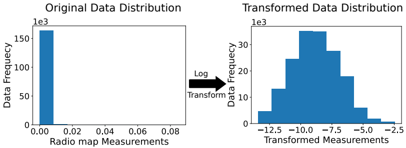


**Dithering:**

- $\underline{\boldsymbol{V}}$ is noise tensor with i.i.d sample from $\mathcal{N}(0, \sigma^2)$.

**Quantize:**

- $\mathcal{G}(\cdot)$ is the quantizer and $\{b_q\}_{q=1}^{Q}$ are quantization bins.

# Dithering

- Adding artificial i.i.d noise before quantization is called dithering [Schuchman 1964].
- Undithered quantized signals has larger errors near quantization bin boundaries, leading to unwanted artifacts.

Original | Monochromatic undithered | Monochromatic dithered

src: https://dev.to/shadowfaxrodeo/why-your-site-should-be-using-dithered-images-3bad

- Dithering evenly distribute the quantization errors making them i.i.d.
  - It was shown that this helps in reducing unnecessary artifacts [Lipshitz et al. 1992].
  - Also, allows equal weighting of i.i.d. errors, simplifying the estimation process [Bhaskar 2016; Cao et al. 2015; Davenport et al. 2014].

# Maximum Likelihood Estimation Formulation

**At fusion center:**

- Fusion center receives set of quantized measurements $\{\underline{\boldsymbol{Y}}(i,j,:)\}_{(i,j)\in\boldsymbol{\Omega}}$.

$$\underline{\boldsymbol{Y}}(i,j,k) = q, \quad \text{w.p.} \quad f_q(\underline{\boldsymbol{M}}(i,j,k)), \quad \forall (i,j) \in \boldsymbol{\Omega}, \; q \in \{1,...,Q\}$$

where,

- transformed measurements $\underline{\boldsymbol{M}}(i,j,k) = h(\underline{\boldsymbol{X}}(i,j,k))$,
- probability distribution function,

$$\begin{aligned} f_q(\underline{\boldsymbol{M}}(i,j,k)) &= \mathbb{P}(\underline{\boldsymbol{Y}}(i,j,k) = q \mid \underline{\boldsymbol{M}}(i,j,k)) \\ &= \Phi(b_q - \underline{\boldsymbol{M}}(i,j,k)) - \Phi(b_{q-1} - \underline{\boldsymbol{M}}(i,j,k)), \end{aligned}$$

and $\Phi$ is the cumulative distribution function of the $\mathcal{N}(0,\sigma^2)$.

**Maximum Likelihood Estimation:**

$$F_{\boldsymbol{\Omega},\underline{\boldsymbol{Y}}}(\boldsymbol{S},\boldsymbol{C}) = -\sum_{(i,j)\in\boldsymbol{\Omega}} \sum_{k=1}^{K} \sum_{q=1}^{Q} \mathbb{1}_{\underline{\boldsymbol{Y}}(i,j,k)=q} \log\big(f_q\big(h([\sum_{r=1}^{R} \boldsymbol{S}_r \circ \boldsymbol{c}_r]_{i,j,k})\big)\big),$$

# DGM for Quantized Measurement

**Quant-SC DGM:**

$$\underset{\boldsymbol{Z},\boldsymbol{C}}{\text{minimize}} - \sum_{(i,j)\in\boldsymbol{\Omega}} \sum_{k=1}^{K} \sum_{q=1}^{Q} \mathbb{1}_{\underline{\boldsymbol{Y}}(i,j,k)=q} \log\left(f_q\left(h([\sum_{r=1}^{R} \boldsymbol{S}_r \circ \boldsymbol{c}_r]_{i,j,k})\right)\right),$$

subject to $\boldsymbol{C} \geq 0.$

where, $\boldsymbol{S}_r = \boldsymbol{g_\theta}(\boldsymbol{z}_r)$ and $\boldsymbol{Z} = [\boldsymbol{Z}_1, \ldots, \boldsymbol{Z}_R]$.

- Needs training data.
- Can work on heavy shadowing.

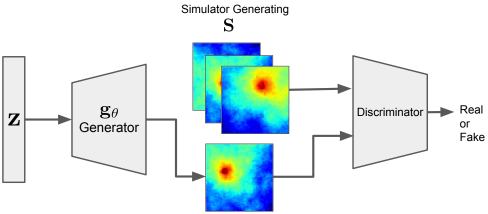


Generative Adversial Network (GAN) as DGM.

## BTD for Quantized Measurement

**Quant-SC BTD:**

$$\underset{\boldsymbol{A},\boldsymbol{B},\boldsymbol{C}}{\text{minimize}} - \sum_{(i,j)\in\boldsymbol{\Omega}} \sum_{k=1}^{K} \sum_{q=1}^{Q} \mathbb{1}_{\underline{\boldsymbol{Y}}(i,j,k)=q} \log\Big(f_q\Big(h\big([\sum_{r=1}^{R} \boldsymbol{S}_r \circ \boldsymbol{c}_r]_{i,j,k}\big)\Big)\Big),$$

subject to $\boldsymbol{A} \geq 0, \; \boldsymbol{B} \geq 0, \; \boldsymbol{C} \geq 0.$

where,

- $\boldsymbol{S}_r = \boldsymbol{A}_r \boldsymbol{B}_r^\top$,
- $\boldsymbol{A} = [\boldsymbol{A}_1, \ldots, \boldsymbol{A}_R]$ and $\boldsymbol{B} = [\boldsymbol{B}_1, \ldots, \boldsymbol{B}_R]$ and $\boldsymbol{C} = [\boldsymbol{c}_1, \ldots, \boldsymbol{c}_R]$.
- Struggle to work in heavy shadowing scenario but doesn't need any training data.

# Recoverability Analysis

## Theorem (Informal)

*Assume that,* **DGM***: Lipschitz continuous or* **BTD***: radio map is low rank, and observations in $\boldsymbol{\Omega}$ ( size $|\boldsymbol{\Omega}| = N$) is uniformly sampled with replacement.*

*With probability at least $1 - 2\delta$, the following holds:*

$$\underbrace{\frac{\|\underline{\boldsymbol{X}}^{\star} - \underline{\boldsymbol{X}}^{\natural}\|_{\mathrm{F}}^2}{IJK}}_{\mathrm{MSE}} \leq \frac{8C_1C_2(1+\tau)}{K}\sqrt{\frac{R}{N}} + C_1\sqrt{\frac{\log(\frac{1}{\delta})}{2N}} + C_1\sqrt{\frac{8\log(\frac{2}{\delta})}{N}} + C_1C_2\nu,$$

*where,*

- $\underline{\boldsymbol{X}}^{*}$ *is an optimal solution from DGM or BTD,*
- $\underline{\boldsymbol{X}}^{\natural}$ *is ground truth radio map,*
- $C_1$ *and* $C_2$ *are constants that depends on transformation function and dithering.*

- Error due to approximation error $\nu$ due to DGM or BTD
- $\tau$ is the model complexity related to,
  - **DGM:** width and depth of neural network,
  - **BTD:** rank of SLF.

- Trade-off between approximation error and model complexity.
- Sample complexity error $O(1/\sqrt{N})$.

# Settings for Simulated Data

**Data Generation:**

- $I = J = 51$ i.e. $51 \times 51$ SLF, $K = 64$ frequency bins.
- SLFs are generated following the joint path loss and log-normal shadowing model from [Goldsmith 2005].
- Two key parameters in above model,
  - variance $\eta^2$, shadowing $\uparrow$ if $\eta^2 \uparrow$, and
  - decorrelation distance $X_c$, shadowing $\uparrow$ if $X_c \downarrow$.
- PSDs are generated as sum of randomly scaled sinc functions [Shrestha et al. 2022; Zhang et al. 2020].

**DGM model:**

- Trained generative adversial network (GAN) on 500,000 samples of SLF on various settings.
- Dimension of latent embedding $D = 256$.

**BTD model:**

- Rank of the SLF, $L$ is set to be 10.

# Baselines and Evaluation Metrics

**Baselines:**

- DowJons [Shrestha et al. 2022] uses DGM but uses real-valued measurements.
- BTD [Zhang et al. 2020] uses BTD but use real-valued measurements.
- Kernel regression (KR) [Romero et al. 2017] assumes the PSD of emitter is known.

**Evaluation Metrics:**

- Log-domain normalized reconstruction error (LNRE) for evaluation,

$$\mathrm{LNRE} = \frac{\|\widehat{\underline{\boldsymbol{M}}} - \underline{\boldsymbol{M}}^{\natural}\|_{\mathrm{F}}^2}{\|\underline{\boldsymbol{M}}^{\natural}\|_{\mathrm{F}}^2}, \tag{5}$$

where $\underline{\boldsymbol{M}} = h(\underline{\boldsymbol{X}})$ is the log-version of $\underline{\boldsymbol{X}}$.

# Visual Results

## Low shadowing scenario

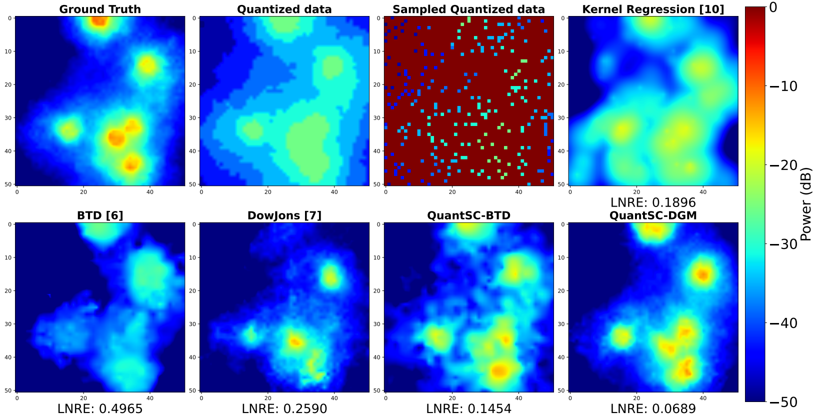


Visualization at the 20th frequency bin; 3-bit quantization, $10\%$ samples, $X_c = 60$, $\eta = 5$.

# Visual Results

## Heavy shadowing scenario

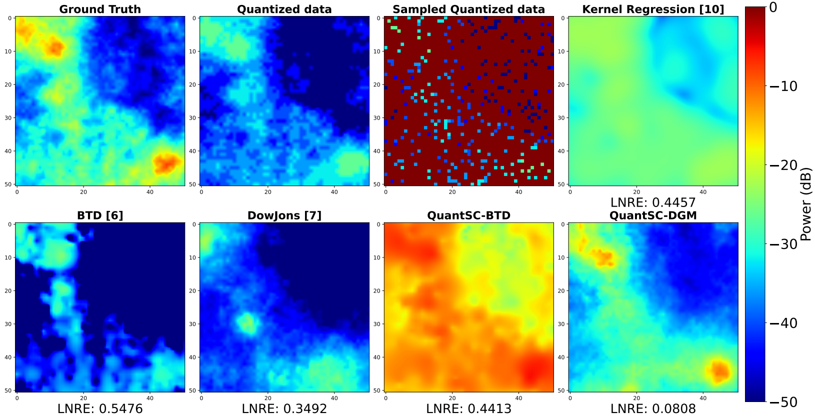


Visualization at the 20th frequency bin; 3-bit quantization, $10\%$ samples, $X_c = 40$, $\eta = 8$.

# Real Data Experiments Settings

**Data Description:**

- CRAWDAD dataset mannheim (v.2008-04-11) [King et al. 2008].
- Indoor floor of $34 \times 14\mathrm{m}^2$ divided into $1 \times 1\mathrm{m}^2$ grids.
- 166 grids with sensors installed at center, 9 frequency bands, unknown R.

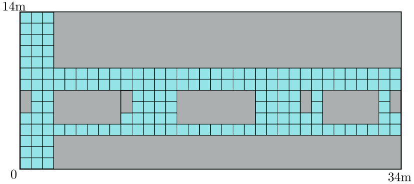


Geometry of the $34 \times 14\mathrm{m}^2$ indoor region. Source: [Shrestha et al. 2022].

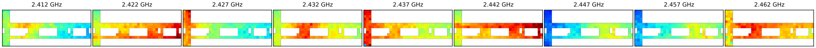


Radio map.

# Visual Results

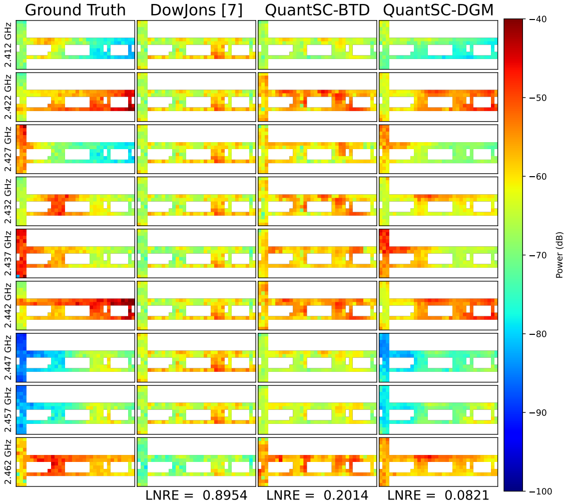


Reconstructed radio map; $3$-bit quantization $10\%$ samples.

# Conclusion

- Proposed MLE framework effectively addresses quantization.
- Framework is compatible with both BTD-based approach which is training free and DGM-based approach which has resilience to heavy shadowing.
- Recoverability of framework has been characterized under imperfect modeling and heavily down-sampled measurements.
- Simulation and real-data experiments demonstrates the effectiveness of the method.

This talk is based on


- **Timilsina, Subash**, Sagar Shrestha, and Xiao Fu. "Deep spectrum cartography from quantized measurements". (Accepted) IEEE ICASSP 2023.
- **Timilsina, Subash**, Sagar Shrestha, and Xiao Fu. "Quantized Radio Map Estimation Using Tensor and Deep Generative Models". [**Accept under mandatory minor revisions**] in IEEE Transactions on Signal Processing.

# Reference I


[1] Sheryl Ball et al. "Consumer applications of cognitive radio defined networks". In: *First IEEE International Symposium on New Frontiers in Dynamic Spectrum Access Networks, 2005. DySPAN 2005.* IEEE. 2005, pp. 518–525.

[2] Juan Andrés Bazerque et al. "Group-lasso on splines for spectrum cartography". In: *IEEE Trans. Signal Process.* 59.10 (2011), pp. 4648–4663.

[3] Sonia A Bhaskar. "Probabilistic low-rank matrix completion from quantized measurements". In: *The Journal of Machine Learning Research* 17.1 (2016), pp. 2131–2164.

[4] Suzhi Bi et al. "Engineering radio maps for wireless resource management". In: *IEEE Wirel. Commun.* 26.2 (2019), pp. 133–141.

[5] Gabriele Boccolini et al. "Wireless sensor network for spectrum cartography based on kriging interpolation". In: *Proc. IEEE PIMRC.* 2012, pp. 1565–1570.

[6] Yang Cao et al. "Categorical matrix completion". In: *Proc. IEEE CAMSAP.* 2015, pp. 369–372.

# Reference II


[7] Mark A Davenport et al. "1-bit matrix completion". In: *Information and Inference: A Journal of the IMA* 3.3 (2014), pp. 189–223.

[8] Xiao Fu et al. "A factor analysis framework for power spectra separation and multiple emitter localization". In: *IEEE Trans. Signal Process.* 63.24 (2015), pp. 6581–6594.

[9] Xiao Fu et al. "Power spectra separation via structured matrix factorization". In: *IEEE Trans. Signal Process.* 64.17 (2016), pp. 4592–4605.

[10] Navid Ghadermarzy et al. "Learning tensors from partial binary measurements". In: *IEEE Trans. Signal Process.* 67.1 (2018), pp. 29–40.

[11] Andrea Goldsmith. *Wireless communications*. Cambridge University Press, 2005.

[12] Mohamed Hamid et al. "Non-parametric spectrum cartography using adaptive radial basis functions". In: *Proc. IEEE ICASSP*. 2017, pp. 3599–3603.

[13] Xu Han et al. "A power spectrum maps estimation algorithm based on generative adversarial networks for underlay cognitive radio networks". In: *Sensors* 20.1 (2020), p. 311.

# Reference III


[14] Arian Houshmand et al. "Eco-routing of plug-in hybrid electric vehicles in transportation networks". In: *2018 21st International Conference on Intelligent Transportation Systems (ITSC)*. IEEE. 2018, pp. 1508–1513.

[15] Marko Höyhtyä et al. "Application of cognitive radio techniques to satellite communication". In: *2012 IEEE International Symposium on Dynamic Spectrum Access Networks*. IEEE. 2012, pp. 540–551.

[16] Beeshanga Abewardana Jayawickrama et al. "Improved performance of spectrum cartography based on compressive sensing in cognitive radio networks". In: *Proc. IEEE ICC*. 2013, pp. 5657–5661.

[17] Seung-Jun Kim et al. "Cognitive radio spectrum prediction using dictionary learning". In: *Proc. IEEE GLOBECOM*. 2013, pp. 3206–3211.

[18] Thomas King et al. *CRAWDAD dataset mannheim/compass (v. 2008-04-11)*. Downloaded from `https://crawdad.org/mannheim/compass/20080411`. Apr. 2008.

[19] Aritra Konar et al. "Parametric frugal sensing of power spectra for moving average models". In: *IEEE Trans. Signal Process.* 63.5 (2014), pp. 1073–1085.

# Reference IV


[20] Chanwoo Lee et al. "Tensor denoising and completion based on ordinal observations". In: *Proc. ICML*. PMLR. 2020, pp. 5778–5788.

[21] Baohua Li et al. "Tensor completion from one-bit observations". In: *IEEE Trans. Image Process.* 28.1 (2018), pp. 170–180.

[22] Stanley P Lipshitz et al. "Quantization and dither: A theoretical survey". In: *Journal of the audio engineering society* 40.5 (1992), pp. 355–375.

[23] LuxCarta. *Wireless Technology And RF Maps*. 2023. URL: https://luxcarta.com/markets/geodata-rf-wireless/.

[24] Gonzalo Mateos et al. "Spline-based spectrum cartography for cognitive radios". In: *Proc. IEEE Conf. Rec. Asilomar Conf. Signals Syst.* 2009, pp. 1025–1029.

[25] Nicolas Maurand et al. "Prototype for the optimization of CO2 injection wells placement in a reservoir". In: *Energy Procedia* 63 (2014), pp. 3097–3106.

[26] Peter McCullagh. "Regression models for ordinal data". In: *Journal of the Royal Statistical Society: Series B (Methodological)* 42.2 (1980), pp. 109–127.

# Reference V


[27] Omar Mehanna et al. "Frugal sensing: Wideband power spectrum sensing from few bits". In: *IEEE Trans. Signal Process.* 61.10 (2013), pp. 2693–2703.

[28] RemCom. *Wireless InSite*. 2023. URL: https://www.remcom.com/wireless-insite-em-propagation-software.

[29] Daniel Romero et al. "Learning power spectrum maps from quantized power measurements". In: *IEEE Trans. Signal Process.* 65.10 (2017), pp. 2547–2560.

[30] Leonard Schuchman. "Dither signals and their effect on quantization noise". In: *IEEE Trans. Commun. Technol.* 12.4 (1964), pp. 162–165.

[31] Sagar Shrestha et al. "Deep Spectrum Cartography: Completing Radio Map Tensors Using Learned Neural Models". In: *IEEE Trans. Signal Process.* 70 (2022), pp. 1170–1184.

[32] ITS: The Nation's Spectrum et al. *Legacy Radio Propagation Software*. 2023. URL: https://www.fcc.gov/about-fcc/what-we-do.

[33] ITS: The Nation's Spectrum et al. *Legacy Radio Propagation Software*. 2023. URL: https://its.ntia.gov/research-topics/radio-propagation-software/radio-propagation-software.

# Reference VI

[34] Yves Teganya et al. "Data-driven spectrum cartography via deep completion autoencoders". In: *Proc. IEEE ICC*. 2020, pp. 1–7.

[35] Guoyong Zhang et al. "Spectrum cartography via coupled block-term tensor decomposition". In: *IEEE Trans. Signal Process.* 68 (2020), pp. 3660–3675.

Questions ?